Key Engineering Materials Vols. 270-273 (2004) pp. 75-81
online at http://www.scientific.net

Non-destructive Determination of Flow Properties through Analysis of Contact Characteristics Beneath Indenter

Sung-Hoon Kim[1], Min-Kyung Baik[1] and Dongil Kwon[1]

[1]School of Materials Science & Engineering, Seoul National University, San 56-1, Sillim-dong, Gwanak-gu, Seoul, 151-742, Korea

Keywords: Continuous Indentation Technique, Flow Properties, Contact Characteristics, FEA, Indentation Load-depth Curve, Work-hardening Exponent, Yield Ratio

Abstract. The continuous indentation technique is widely used for nondestructive evaluation of the mechanical properties of devices and materials. In particular, flow properties can be obtained by using this technique with a spherical indenter. To obtain accurate flow properties, however, contact characteristics such as the contact area or depth between material and indenter must be determined precisely. In this study, contact characteristics were determined by analysis of the contact morphology and stress-strain distribution from FEA (finite-element analysis) using mechanical property data for several steels. The contact characteristics obtained from FE simulation were compared to an analysis of the parameters of indentation load-depth curves for the steels. The contact characteristics were determined as functions of such parameters as work-hardening exponent and indentation depth. The flow properties were evaluated by analysis of indentation morphology for 18 materials on the basis of pre-existing definitions of stress and strain, and the definitions were verified by comparison of the flow properties with tensile testing data.

Introduction

Flow properties such as yield and tensile strength, and work-hardening exponent, etc. are widely used as basic design information on materials strength and as an acceptance test for materials specification. Tension tests, in which a standard specimen is subjected to a continually increasing uniaxial tensile force and specimen elongation is observed, are generally used to evaluate flow properties. However, tension tests cannot be used for safety inspection of structural units because the specimen must be removed, which may cause failure or fracture.

The continuous indentation method has been actively studied as a method for evaluating the flow properties of structural units as well as materials. In continuous indentation tests, the load applied and the depth penetrated into the object by an indenter are continuously measured and represented as an *indentation load-depth curve*. Through analysis of this curve, various mechanical properties, such as flow properties, residual stress, fracture properties, viscoelastic properties, hardness, etc., can be evaluated. In particular, flow properties can be evaluated through the continuous indentation technique by using a spherical indenter. To evaluate flow properties exactly, however, such contact characteristics as the contact area or depth between material and indenter must be determined precisely, and this cannot be done under maximum load in actual indentation testing.

In this study the contact characteristics were determined by FEA based on conditions that accurately reflect the conditions of actual indentation tests. The contact characteristics determined from FEA were compared with previous research reporting these characteristics as functions of the material properties.

Theoretical Background

Indentation Load-Depth Curve. The indentation load-depth curve is obtained from continuous indentation test, as shown in Fig. 1. The single indentation load-depth curve in Fig. 1(a) includes one loading curve and one unloading curve. The maximum depth h_{max} is the total displacement of the

material and the indenter at maximum load P_{max} including elastic and plastic deformation. In unloading, the elastic deformation is fully recovered and the initial slope of the unloading curve is the indentation stiffness of the specimen and the indenter, S [1,2]. Thus the final depth h_f is the plastic deformation of the material.

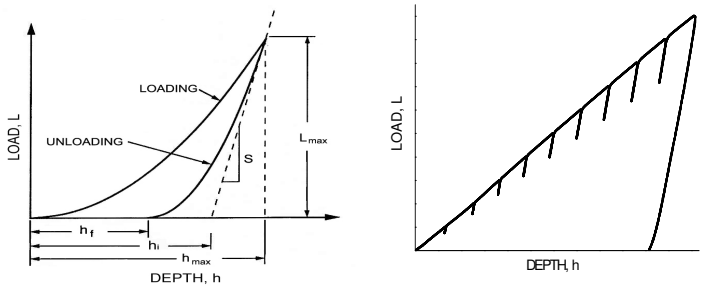

(a) (b)

Fig. 1. Indentation load-depth curves: (a) single and (b) multiple indentation curve.

Doerner and Nix [2] showed that elastic modulus could be evaluated by this test, and Oliver and Pharr [1] established a method to evaluate elastic modulus and load-on hardness. However, work is ongoing to evaluate other mechanical properties such as fracture toughness [3,4], flow properties [5,6], viscoelastic properties [7,8] and residual stress [9,10]. Among these properties, methods for evaluating flow properties are of interest in some industrial fields because they can be used for materials with local property gradients and for materials in service.

Evaluation of Indentation Flow Properties. Indentation flow properties are the properties obtained from analysis of the indentation load-depth curve. This technique starts from the premise that materials behave similarly in the tensile and compressive loading state. The flow curves of many materials in the uniform plastic deformation region can be expressed by the following simple power-curve relation:

$$\sigma = K\varepsilon^n \tag{1}$$

where σ is the true stress, ε is the true strain, n is the work-hardening exponent and K is the strength coefficient. The strain is a dimensionless parameter describing a fractional change in shape. The shape is determined by the ratio d/D, where d is the chordal indentation diameter and D is the indenter diameter. The flow strain ε has been expressed as a percentage strain by Tabor [11]:

$$\varepsilon = 0.2\frac{d}{D} = 0.2\sin\gamma, \tag{2}$$

where γ is half of contact angle between material and ball indenter. Since the maximum strain that can be obtained from Eq. (2) is 0.2, this equation has the limitation that it cannot be used to describe the flow strain for materials with very large strain or elongation. Ahn et al. suggested a new equation based on the idea that the displacement of the indenter-penetration direction can be obtained from the geometrical shape of the indenter and the strain can be obtained by differentiation of the displacement relation [5]:

$$\varepsilon = \frac{\alpha}{\sqrt{1-(d/D)^2}}\frac{d}{D} = \alpha\tan\gamma, \tag{3}$$

where α is a constant, generally 0.12.

The flow stress can be obtained from the relation with the mean contact pressure P_m defined as

$$P_m = \frac{L}{A_c}, \tag{4}$$

where L is the applied load and A_c, the contact area between indenter and material, is a function of d. The relation can be expressed, with the introduction of the plastic constraint factor ψ, as [4, 5, 11, 12]:

$$\sigma = \frac{P_m}{\psi}, \tag{5}$$

where ψ is a value changing with deformation characteristics: elastic, elastoplastic, and fully plastic.

Determination of the Contact Area (or Depth). The contact area A_c is a function of d and d is a function of the contact depth h_c. The contact depth is thus the basic datum for determining such flow properties as stress and strain. The contact depth is, however, difficult to obtain due to the elastic deflection and plastic deformation of material around the indenter, as shown in Fig. 2. Plastic deformation occurs in two forms, pile-up (Fig. 2(a) and sink-in (Fig. 2(b); the contact area between the material and indenter is increased by pile-up but decreased by sink-in.

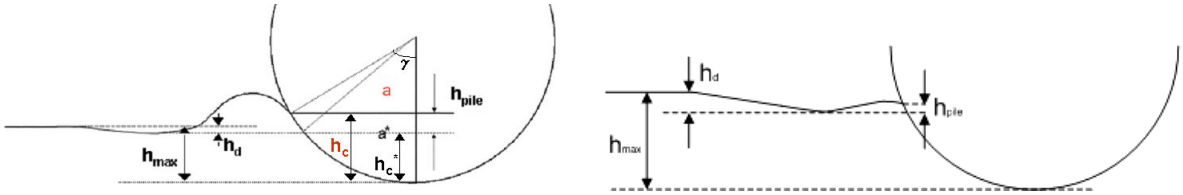

(a) (b)

Fig. 2. Deformation phenomena around the indenter; (a) pile-up and (b) sink-in

The elastic deflection decreases the contact area and amount of the deflection. The following equation has been suggested for the deflection depth h_d [1]:

$$h_d = \omega \frac{L_{max}}{S}, \tag{6}$$

where S is stiffness, the initial slope of the unloading curves, and ω is a constant related to the shape of the indenter. Using the depth relation, Oliver and Pharr [1] suggested that

$$h_c^* = h_{max} - h_d, \tag{7}$$

where h_c^* is the contact depth ignoring the pile-up and sink-in phenomena. The increase or decrease in the contact area by plastic deformation is known to be a function of the work-hardening exponent, the ratio of yield strength to elastic modulus and the ratio of the penetration depth to the indenter radius [13-17]. Early research on the phenomena studied primarily the effect of the work-hardening exponent. Norbury and Samuel suggested that amount of pile-up or sink-in could be expressed as a percentage of the depth and the percentage pile-up or sink-in constants were related to the work-hardening exponent [15]. Early research led to the following relationship between the amount of pile-up or sink-in and the work-hardening exponent [16, 17]:

$$\frac{s}{h_{max}} = \frac{1}{2}\left(\frac{2+n}{2}\right)^{2\left(\frac{1}{n}-1\right)} - 1 \tag{8}$$

$$\frac{s}{h_{max}} = \frac{5}{2}\left(\frac{2-n}{4+n}\right) - 1 \tag{9}$$

where s, the amount of pile-up or sink-in, can be expressed as h_{pile} - h_d , as shown in Fig. 2 (a). On the basis of these results, the contact depth h_c for pile-up can be expressed as

$$h_c = h_{max} - h_d + h_{pile}, \tag{10}$$

where h_{pile} is the pure amount of pile-up considering elastic deflection. Finally, the contact area is defined from the geometrical relation of the contact area and contact depth:

$$A_c = \pi a^2 = \pi\left(2Rh_c - h_c^2\right), \tag{11}$$

where a is the contact radius and R is the radius of the spherical indenter. However, recent research has found that the amount of pile-up or sink-in is a function not only of the work-hardening exponent but also of various other parameters such as the ratio of yield strength to elastic modulus and the ratio of penetration depth to indenter radius, and the need to consider these additional parameters has made it more complex to determine the contact area [13,18]. The research to consider the effects has been performed by FEA, but the effects have not been quantified like the effect of n.

Experimental Procedure

Continuous Indentation Test. The materials tested were the 17 industrial steels and the one aluminum alloy shown in Table 1. The specimens were cut to 25×25×20 mm, ground, and polished with 1 μm alumina. Continuous indentation tests were performed for each material using Frontics, Inc.'s AIS2000 equipment with a spherical indenter of 0.5 mm radius made of WC. Each experimental condition was selected as: loading or unloading rate 0.3 mm/min, maximum indentation depth 250 μm, number of unloadings 10 and unloading rate 30%.

Finite Element Analysis. Simulation of the indentation process was performed using ABAQUS finite element code. An axisymmetric FE analysis was employed with the indenter modeled as a rigid spherical ball. A cylindrical specimen of diameter 200 mm and height 100 mm was modeled with 3738 linear four-node elements; indenter diameter was 1 mm. The indentation depth was selected as 250 μm, as in the indentation test. A cylindrical coordinate system with radial coordinate r and axial coordinate z was used. The bottom surface of the specimen has the z displacement fixed, whereas free movement is allowed in the r direction. The appropriate boundary conditions for modeling the axisymmetric behavior were applied along the centerline, and a free surface was modeled at the top and outside surface of the specimen. A friction coefficient of 0.2 was used in the computations to model the behavior of the indenter/specimen interface. The basic input material properties were true stress-true strain points, elastic modulus and Poisson's ratio for each material. Tensile properties were measured from tension tests using the Instron 5582 on the basis of ASTM E8-00. Elastic modulus and Poisson's ratio were measured by the ultrasonic method using Tektronics, Inc.'s TDS220.

Table 1. Materials used in this study.

Material	Al2011	API X42	API X65	KP	NAK	SA508
	Aluminum Alloy	Pipe Steel	Pipe Steel	Pipe Steel	Plastic Mold steel	Pressure Vessel Steel
	SCM21	SCM440	S45C	SK3	SK4	SKD11
	Structural Steel	Structural Steel	Structural Steel	Tool Steel	Tool Steel	Tool Steel
	SKD61	SKH51	SS400	SUJ2	SUS304	SUS316
	Tool Steel	Tool Steel	Structural Steel	Bearing Steel	Stainless Steel	Stainless Steel

Results and Discussion

By using simulation conditions reflecting the actual state of the indentation by inputting stress-strain points from tensile testing, indentation morphologies and indentation load-depth curves were obtained by FE simulation for 18 materials. Figure 3 shows that indentation load-depth curves from FE simulation were very similar to those from continuous indentation tests, so that the results of indentation morphology obtained from FE simulation are considered reliable.

Title of Publication (to be inserted by the publisher)

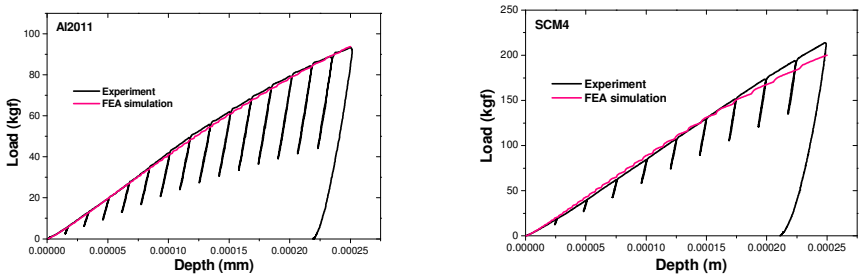

Fig. 3. Indentation load-depth curves from continuous indentation tests and from FE simulation.

Determination of Contact Area Considering Pile-up. It was observed from the simulation results for 18 materials that pile-up height was dependent on indentation depth and work-hardening exponent. This is shown in Figure 4 for the materials used here with work-hardening exponents from 0 to 0.4.

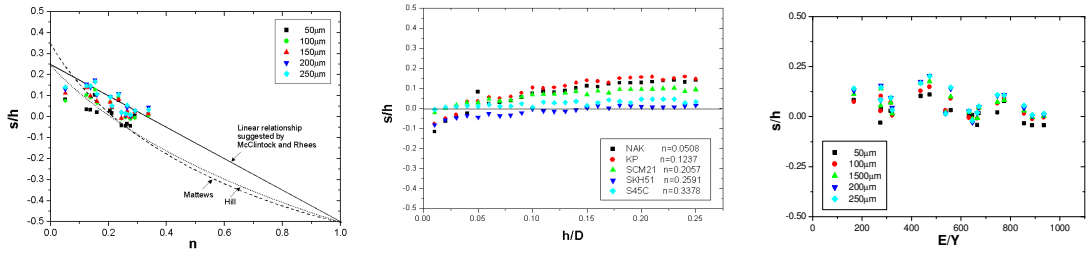

(a) (b) (c)

Fig. 4. Correlations between the pile-up parameter and (a) *n,* (b) *h/D* and (c) *E/Y*.

Here *s/h* is the pile-up parameter, where *s* is the pile-up height from the original plane and *h* is the depth of penetration into specimen from the original plane. For small indentation depths, the relation between *s/h* and *n* is described well by the equation (9) suggested by Hill. However, the relation deviates from this equation with increasing depth and shows a linear inverse proportion: for indentation depths over 200 μm, the relationship suggested by Hill is not suited to metallic materials having *n* less than 0.4, but the linear relationship suggested by Rhee and McClintock works well. Also, the *s/h* increased with increasing indentation depth, as shown in Figure 4 (b); this figure also shows that pile-up did not occur clearly in the indentations for materials with large *n*.

On the other hand, the pile-up parameter either was not related to the yield ratio *E/Y* or was in somewhat inverse proportion to it, as shown in Figure 4 (c). It is thus confirmed that a new relationship must be suggested as a function of indentation depth and that this new relationship must be used, in addition to that for the work-hardening exponent suggested by Hill, Mattews and McClintock, in order to determine the precise contact depth (or area).

Derivation of Flow Stress and Strain. In this study the contact area was directly measured from the contact morphology between the indenter and the material, obtained from FE simulation. As discussed above, several equations have been suggested to express the stress and strain value. Of these, two equations suggested by Tabor and Ahn were verified in this study, since the definitions of stress are very similar. For nine representatives of our 18 materials, the stress-strain results evaluated by FE simulation morphology were compared with those evaluated by tension test. The results are superposed in Figure 5 and generally the results using Tabor's equations agreed better with the tensile results than those using Ahn's equations. The results using Tabor's equations described work-hardening behavior similar to that of the actual material. However, Tabor's definition of strain has the limitation that cannot express strain values over 0.2 (when indentation is performed to the same depth as indenter radius *R*). Therefore, to apply Tabor's equation to materials having large strain values, the strain over 0.2 must be extrapolated. The results from the equation suggested by Ahn didn't show better result on the tensile results than Tabor's equation. However, this definition of

strain can express strain values larger than 0.2. In addition, for stainless steel, Ahn's definition reflected the flow characteristics of the materials under large strain.

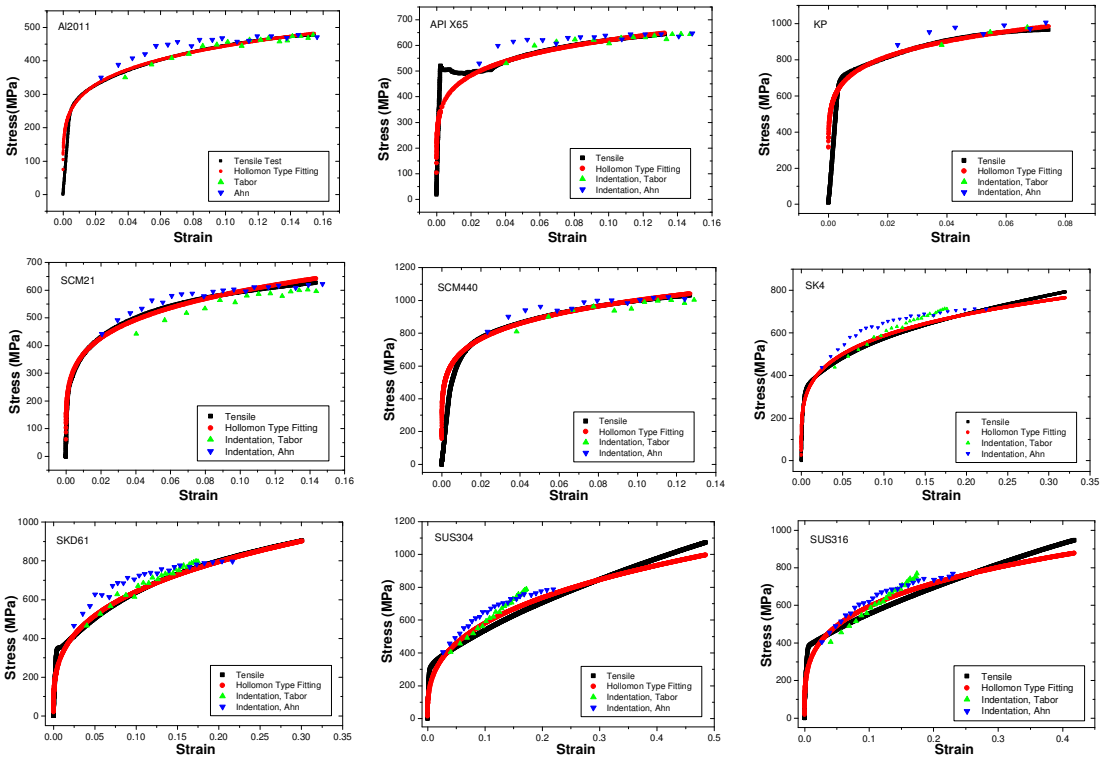

Fig. 5. Comparison of flow properties from indentation tests and those from tensile tests.

The stress and strain values obtained here by the two definitions from the FE simulation results showed Hollomon-type work-hardening behavior, probably because the definitions were suggested on the basis of such behavior. Therefore, in order to describe accurately the work-hardening behavior of materials with non-Hollomon-type behavior, the two definitions must be revised. Further research will make possible either the suggestion of a new equation or revision of existing equations.

Summary

Research on evaluating the flow curves of materials and structural units has used the continuous indentation technique with a spherical indenter, and contact characteristics must be analyzed to do this precisely. However, since it is difficult to measure the contact characteristics directly, in this study FE simulation was used, with tensile testing results for real materials used as the basic simulation data. Contact morphologies and load-depth curves were obtained from the simulation and previously suggested definitions of stress and strain were verified by analyzing them.

Since contact depth values affect stress and strain values, they must be determined precisely by taking into account indentation morphology. The definitions suggested by such previous researchers as Hill and Matthews are functions of the work-hardening exponent only. The results of this study show that the pile-up parameter changed with increasing indentation depth, so that new definitions including indentation depth as well as work-hardening exponent are needed.

In addition, the definition of stress and strain suggested by Tabor describes work-hardening behavior well but cannot be applied to the behavior of materials having large tensile strains due to the limitation of the maximum value. On the other hand, Ahn's definition can be applied to the work-hardening behavior of materials having large tensile strains, and also can describe the work-hardening behavior of stainless steels.

References

[1] W.C. Oliver and G.M. Pharr: J. Mater. Res. Vol. **7** (1992), p. 1564.

[2] M.F. Doerner and W.D. Nix: J. Mater. Res. Vol. 1 (1986), p. 601.

[3] J. Malzbender and G. de With: Surf. Coat. Tech. Vol. 135 (2000), p. 60.

[4] K.L. Murty, M.D. Mathew and F.M. Haggag: Int. J. Pressure Vessels and Piping Vol. 75 (1998), p. 831.

[5] J.H. Ahn and D. Kwon: J. Mater. Res. Vol. 16 (2001), p. 3170.

[6] F.M. Haggag: *ASTM STP 1204*, Philadelphia (1993), p. 27.

[7] S.A.S. Asif, K.J. Wahl and R.J. Colton: Rev. Sci. Inst. Vol. 70 (1999), p. 2408.

[8] B.N. Lucas, W.C. Oliver and J.E. Swindeman: *MRS Symposium Proceedings* Vol. 522 (1998), p. 3.

[9] S. Suresh and A.E. Giannakopoulos: Acta Mater. Vol. 46 (1998), p. 5755.

[10] Y.H. Lee and D. Kwon: J. Mater. Res. Vol. 17 (2002), p. 901.

[11] D. Tabor: Hardness of Metals (Clarendon Press, Oxford 1951).

[12] H.A. Francis: Trans. ASME, July (1976), p. 272.

[13] B. Taljat, T. Zacharia and G.M. Pharr: *MRS Symposium Proceedings* Vol. 522 (1998), p. 33.

[14] S.S. Rhee and F.A. McClintock: *Proc. 4th US Nat. Conf. Applied Mechanics*, ASME, Berkeley California (1962), p. 1007.

[15] A.L. Norbury and T. Samuel: J. Iron Steel Inst. Vol. 117 (1928), p. 673.

[16] J.R. Matthews: Acta Metal. Vol. 28 (1980), p. 311.

[17] R. Hill, B. Storåkers and A.B. Zdunek: *Proc. R. Soc. London*, A423 (1989), p. 301.

[18] Y.T. Cheng and C.M. Cheng: *Phil. Mag. Lett.*, 78 (1998), p. 115.